SUPPLEMENTARY MATERIAL

Tropomyosin and myosin-II cellular levels promote actomyosin ring assembly in fission yeast

Benjamin C. Stark*, Thomas E. Sladewski*, Luther W. Pollard, & Matthew Lord†

Department of Molecular Physiology & Biophysics
University of Vermont
Burlington, VT 05405.

*These authors contributed equally to the work
†Corresponding author: matthew.lord@uvm.edu; Tel. 802-656-9898; Fax. 802-656-0747.

Running Head: Tropomyosin regulates *S. pombe* myosin-II

Materials and Methods

Fission yeast strains and genetic methods

The strains employed in this study are listed in Supplementary Table S1. Strains were constructed by back-crossing or genomic integrations using homologous recombination (Bahler et al., 1998; Moreno, 1991). To integrate two copies of *YFP-myo2* into a haploid a *myo2*$^{+}$*/myo2Δ::YFP-ura4*$^{+}$ heterozygote diploid (Sladewski et al., 2009) was transformed with the *LEU2*$^{+}$ p*YFP-myo2* plasmid (Sladewski et al., 2009), sporulated, and haploid segregants isolated by random spore analysis. *myo2Δ::YFP-ura4*$^{+}$ haploids harboring p*YFP-myo2* were isolated by screening segregants for growth on EMM-Ura^{-} Leu^{-} plates. A *YFP-myo2* fragment (including the *myo2* terminator) was then amplified from p*YFP-myo2* using 5' YFP and 3' *myo2* terminator cloning primers. The fragment was transformed and integrated into the *myo2Δ::YFP-ura4*$^{+}$ haploid (harboring p*YFP-myo2*) in place of *ura4*$^{+}$. Cells were grown over-night on YE5S plates and then replica-plated to minimal media plates containing 0.1 % 5-fluoroorotic acid (5-FOA) to isolate *ura*$^{-}$ colonies. Most *ura*$^{-}$ colonies no longer carried the p*YFP-myo2* plasmid and possessed an integrated form of *YFP-myo2* (as confirmed by visualization of YFP-labeled contractile rings by fluorescence microscopy and diagnostic PCRs of genomic DNA). A sub-population of the *ura4*$^{-}$ colonies were *LEU2*$^{+}$. However, of all *LEU2*$^{+}$ isolates tested, none harbored p*YFP-myo2* since cells lacked the cytokinesis defects associated with elevated Myo2p expression from this multi-copy plasmid, and yielded 2:2 *leu*$^{-}$:*LEU2*$^{+}$ tetrad progeny upon back-crossing with a wild-type *leu*$^{-}$ haploid. *leu*$^{-}$ progeny from these crosses lacked YFP-labeled contractile rings, whereas the *LEU2*$^{+}$ progeny exhibited YFP-labeled rings that were much brighter than those in *ura*$^{-}$ *leu*$^{-}$ *YFP-myo2* cells. This pattern of segregation indicated that the integrated *LEU2*$^{+}$ marker was linked to the *myo2* locus. The integration of a second copy of *YFP-myo2* originating from the p*YFP-myo2 LEU2*$^{+}$ plasmid was confirmed by diagnostic PCR of genomic DNA.

Plasmids

The plasmids employed in this study are listed in Supplementary Table S2. To construct the pGST-*cdc8* plasmid the *cdc8* ORF was PCR-amplified from a genomic DNA library using 5' *NotI-cdc8*: GCGGCCGCATGGATAAGCTTAGAGAGGTATGAG and 3' *SalI-cdc8*: GTCGA-CCTACAAATCCTCAAGAGCTTGGTGAAC and the iproof DNA polymerase. The fragment was sub-cloned into a TOPO vector, cut with *NotI* and *SalI* and then ligated into *NotI*/*SalI* lineraized pDS473a (*nmt1* inducible promoter, *LEU2* marker). The fidelity of the construct was confirmed by DNA sequencing. p*rlc-ura4*$^{+}$ is a genomic clone spanning the *rlc1* promoter and ORF from a p*UR19* genomic DNA library.

Protein purification

Myo2p was purified as previously described (Lord and Pollard, 2004; Sladewski et al., 2009). Cdc8p was purified following over-expression in fission yeast as a GST-fusion using the maximum-strength *nmt1* inducible promoter. Liquid cultures were grown to saturation in EMM Leu^{-} with 5 μg/ml of thiamine. Cells were harvested and washed three times in EMM Leu^{-} medium and diluted to an optical density at 595 nm (OD_{595}) of ~0.05 in 4 liters of the same medium. Over-expression was achieved by 24–28 hours of growth at 32°C, by which time the OD had reached ~3. Cells were harvested and washed once in water and once in ice-cold lysis buffer (750 mM KCl, 25 mM Tris-HCl, pH 7.4, 4 mM $MgCl_2$, 20 mM $Na_4P_2O_7$, 2 mM EGTA, and 0.1% Triton X-100). Pellets were resuspended in an equal volume of ice-cold lysis buffer

with additives consisting of 1 mM DTT, 4 mM ATP, 2 mM PMSF, and complete EDTA-free protease inhibitors (Roche). Cells were lysed by glass bead beating with a Fastprep bead beater (MP Biochemicals). The lysate was centrifuged at 500 *g* for 5 min to remove unlysed cells and beads and further centrifuged at 100,000 *g* for 45 min to remove insoluble matter. The supernatant was batch incubated with 1.5 ml of glutathione-Sepharose (Amersham Biosciences) for 90 min, and then transferred to a 20 ml column. The bound sample was washed with lysis buffer with additives (4 x 15 ml) and eluted in 5 ml of lysis buffer plus additives and 10 mM glutathione. Following thorough dialysis into A15 buffer (0.5 M KCl, 10 mM imidazole, pH 7.0, 10 mM EDTA, 1 mM DTT, and 0.3 mM NaN_3) the sample was treated with thrombin to detach GST. GST was removed by overnight batch incubation with glutathione-Sepharose followed by 3-4 slow passages of the sample over the same resin after packing it into a column. Flow-through consisted of Cdc8p which was purified then passed over 0.2 ml of benzamidine Sepharose to remove thrombin. Actin was purified from rabbit skeletal muscle acetone powder (Spudich and Watt, 1971). Actin filaments were formed by addition of 50 mM KCl and 1 mM $MgCl_2$.

Supplemental Figures and Legends

Figure S1. Contractile ring dynamics in *cdc8-27* and *myo2-E1* mutants.
Time-lapse images of cells captured every 2 minutes by fluorescence microscopy. The montages compare Rlc1p-GFP/YFP-Myo2p ring dynamics in *myo2-E1*, *cdc8-27*, and *cdc8-27 2xYFP-myo2* strains. Bar: 4 μm. Rings from these series were used to generate kymographs presented in Figure 5A.

Figure S2. *cdc8-27* and *myo2-E1* mutations delay the timing of contractile ring assembly and constriction. Time-lapse series of single cells (A) and their accompanying plots (B) charting ring dynamics (dwell and constriction phases) in relationship to spindle elongation and breakdown during mitosis. A) Time-lapse images of wild-type, *cdc8-27*, and *myo2-E1* cells (captured every 3 minutes for 1 hour in these particular examples) are shown following spindle pole body (SPB) separation. In each case contractile rings are marked by Rlc1p-GFP and SPBs by Sad1p-GFP. B) For each of the representative cells shown in A the timing of contractile ring assembly and constriction is monitored by overlaying ring diameter (filled circles) with corresponding SPB separation distances (diamonds).

Figure S3. Purification of functional fission yeast tropomyosin.
Fission yeast purified Cdc8p binds actin filaments. Lane 1: molecular weight markers. Cdc8p remains in the supernatant following ultracentrifugation in the absence of actin filaments (*left* lanes) and co-pellets with actin filaments (*right* lanes).

Supplementary Movie Legends

Movie 1. Myo2p-driven filament gliding from *in vitro* motility assays using bare actin filaments (*left*) versus Cdc8p-actin filaments (*right*). Myo2p was attached to nitrocellulose-coated cover-slips at a concentration 32 μg/ml. Filaments are labeled with rhodamine-phalloidin. The movies were generated from time-lapse images recorded at 2 s intervals (sped up x20).

Movie 2. As in Movie 1, only Myo2p was attached to cover-slips at 0.8 μg/ml.

Table S1. Fission yeast strains.

Strain	Genotype	Source
MLY 29	*h$^+$/h$^-$ leu1-32/leu1-32 ura4-D18/ura4-D18 ade6-M210/ade6-216 his3-D1/his3-D1 myo2/myo2Δ::^{m}YFP-ura4$^+$*	(Sladewski et al., 2009)
MLY 66	*h$^+$ leu1-32 ura4-D18 ade6 his3-D1 ^{m}YFP-myo2*	(Sladewski et al., 2009)
MLY 140	*h$^+$ leu1-32 ura4-D18 ade6 his3-D1 ^{m}YFP-myo2 sad1-^{m}GFP:kan^R*	This study
MLY 273	*h$^+$ leu1-32 ura4-D18 ade6 his3-D1 2x^{m}YFP-myo2*	This study
MLY 275	*h$^-$ leu1-32 ura4-D18 ade6 his3-D1 2x^{m}YFP-myo2 sad1-^{m}GFP:kan^R*	This study
MLY 402	*h$^-$ leu1-32 ura4-D18 ade6 his3-D1 myp2Δ::his7$^+$ ^{m}YFP-myo2*	(Sladewski et al., 2009)
MLY 400	*h$^+$ leu1-32 ura4-D18 ade6 his3-D1 myp2Δ::his7$^+$ 2x^{m}YFP-myo2*	This study
MLY 463	*h$^-$ leu1-32 ura4-D18 ade6 his3-D1 ^{m}YFP-myo2 rlc1-^{m}CFP: kan^R*	This study
MLY 464	*h$^-$ leu1-32 ura4-D18 ade6 his3-D1 cdc8-27 ^{m}YFP-myo2*	This study
MLY 466	*h$^+$ leu1-32 ura4-D18 ade6 his3-D1 cdc8-27 2x^{m}YFP-myo2*	This study
MLP 319	*h$^-$ leu1-32 ura4-D18 ade6-M216 his3-D1 myo2-E1 rlc1-^{m}GFP:kan^R*	This study
MLY 572	*h$^-$ leu1-32 ura4-D18 ade6-M216 his3-D1 rlc1-^{m}GFP:kan^R sad1-^{m}GFP:kan^R*	This study
MLY 580	*h$^-$ leu1-32 ura4-D18 ade6-M216 his3-D1 cdc8-27 rlc1-^{m}GFP:kan^R sad1-^{m}GFP:kan^R*	This study
MLY 570	*h$^-$ leu1-32 ura4-D18 ade6-M216 his3-D1 myo2-E1 rlc1-^{m}GFP:kan^R sad1-^{m}GFP:kan^R*	This study
MLY 590	*h$^+$ leu1-32 ura4-D18 ade6 his3-D1 cdc8-27 2x^{m}YFP-myo2 sad1-^{m}GFP:kan^R*	This study
MLY 639	*h$^+$ leu1-32 ura4-D18 ade6 his3-D1 2x^{m}YFP-myo2 rlc1-^{m}CFP: kan^R sad1-^{m}GFP:kan^R*	This study
TP 150	*h$^-$ leu1-32*	M. Yanagida
MLY 83	*h$^-$ leu1-32 ura4-D18 nat^R:41nmt1 prom-FLAG-myo2*	(Sladewski et al., 2009)

Table S2. Plasmids.

Plasmid	Comment	Source
p*GST-cdc4*	pDS473a-based (*nmt1* promoter, *LEU2* marker)	(Lord and Pollard, 2004)
p*GST-rlc1*	pDS473a-based (*nmt1* promoter, *ura4*$^+$ marker)	(Lord and Pollard, 2004)
p*GST-cdc8*	pDS473a-based (*nmt1* promoter, *LEU2* marker)	This study
pFA6a-*nat*^{R}*-nmt41prom-FLAG*	pFA-*nat*^{R}*-nmt41prom* with N-terminal FLAG tag	(Sladewski et al., 2009)
KS-ura4	template for gene replacement with *ura4*$^+$	(Bahler et al., 1998)
p*YFP-myo2*	*YFP-myo2* fusion in pDS473a-based vector (*LEU2* marker); includes *myo2* promoter and terminator	(Sladewski et al., 2009)
p*YFP-ura4*$^+$	*myo2* promoter-*YFP-ura4*$^+$*-myo2* terminator cassette in pDS473a-*LEU2* vector; for *YFP-myo2* integrations	(Sladewski et al., 2009)
p*rlc1-ura4*$^+$	*rlc1* genomic clone on a *ura4*$^+$ multi-copy plasmid	This study

References

Bahler, J., J.Q. Wu, M.S. Longtine, N.G. Shah, A. McKenzie, 3rd, A.B. Steever, A. Wach, P. Philippsen, and J.R. Pringle. 1998. Heterologous modules for efficient and versatile PCR-based gene targeting in Schizosaccharomyces pombe. *Yeast*. 14:943-51.

Lord, M., and T.D. Pollard. 2004. UCS protein Rng3p activates actin filament gliding by fission yeast myosin-II. *J Cell Biol*. 167:315-25.

Moreno, S., Klar, A., Nurse, P. 1991. Molecular Genetic Analysis of Fission Yeast *Schizosaccharomyces pombe*. *Methods Enzymol*. 194:795-823.

Sladewski, T.E., M.J. Previs, and M. Lord. 2009. Regulation of fission yeast myosin-II function and contractile ring dynamics by regulatory light-chain and heavy-chain phosphorylation. *Mol Biol Cell*. 20:3941-52.

Spudich, J.A., and S. Watt. 1971. The regulation of rabbit skeletal muscle contraction. I. Biochemical studies of the interaction of the tropomyosin-troponin complex with actin and the proteolytic fragments of myosin. *J Biol Chem*. 246:4866-71.

Stark et al.
Figure S1.

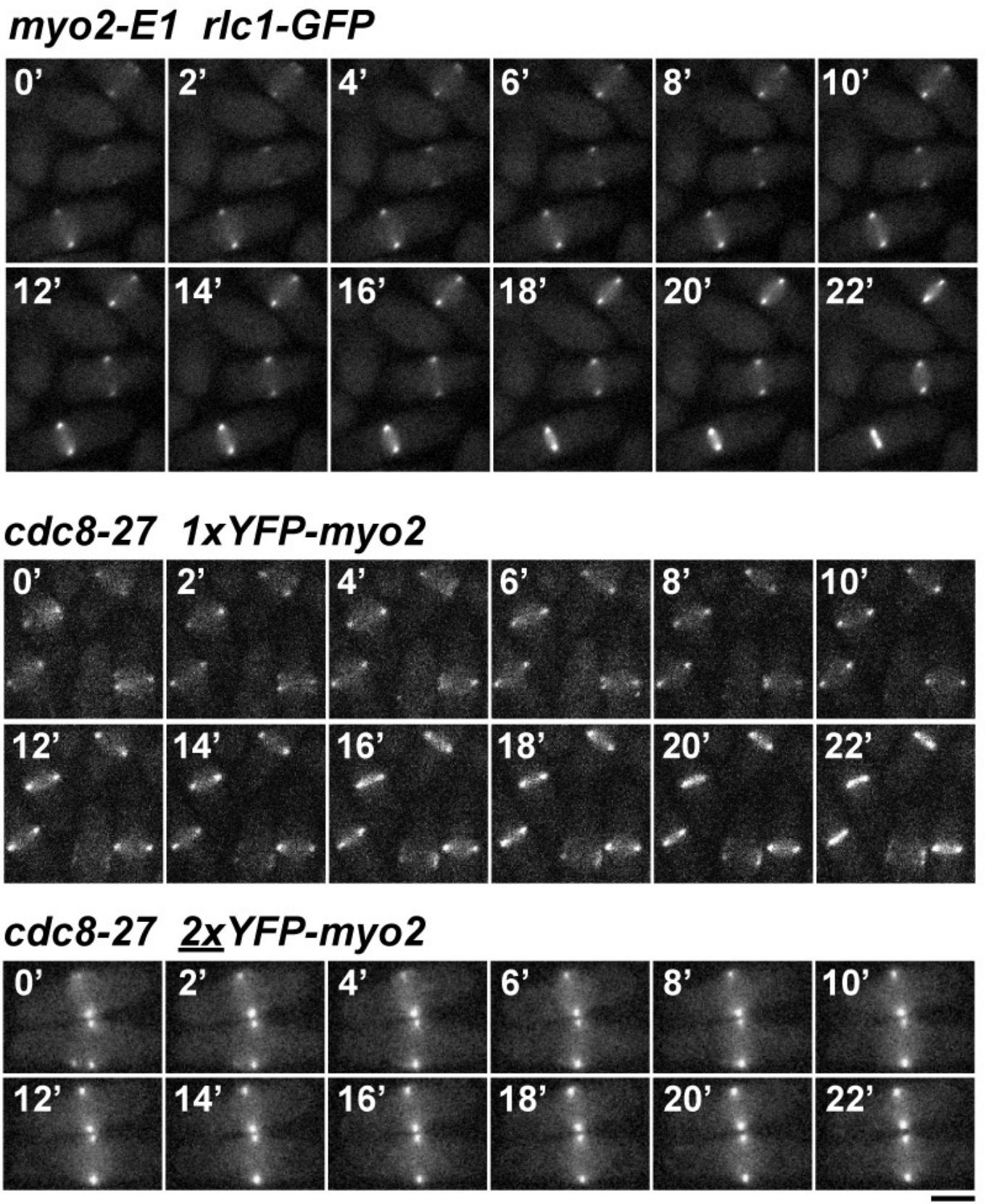

Stark et al.
Figure S2.

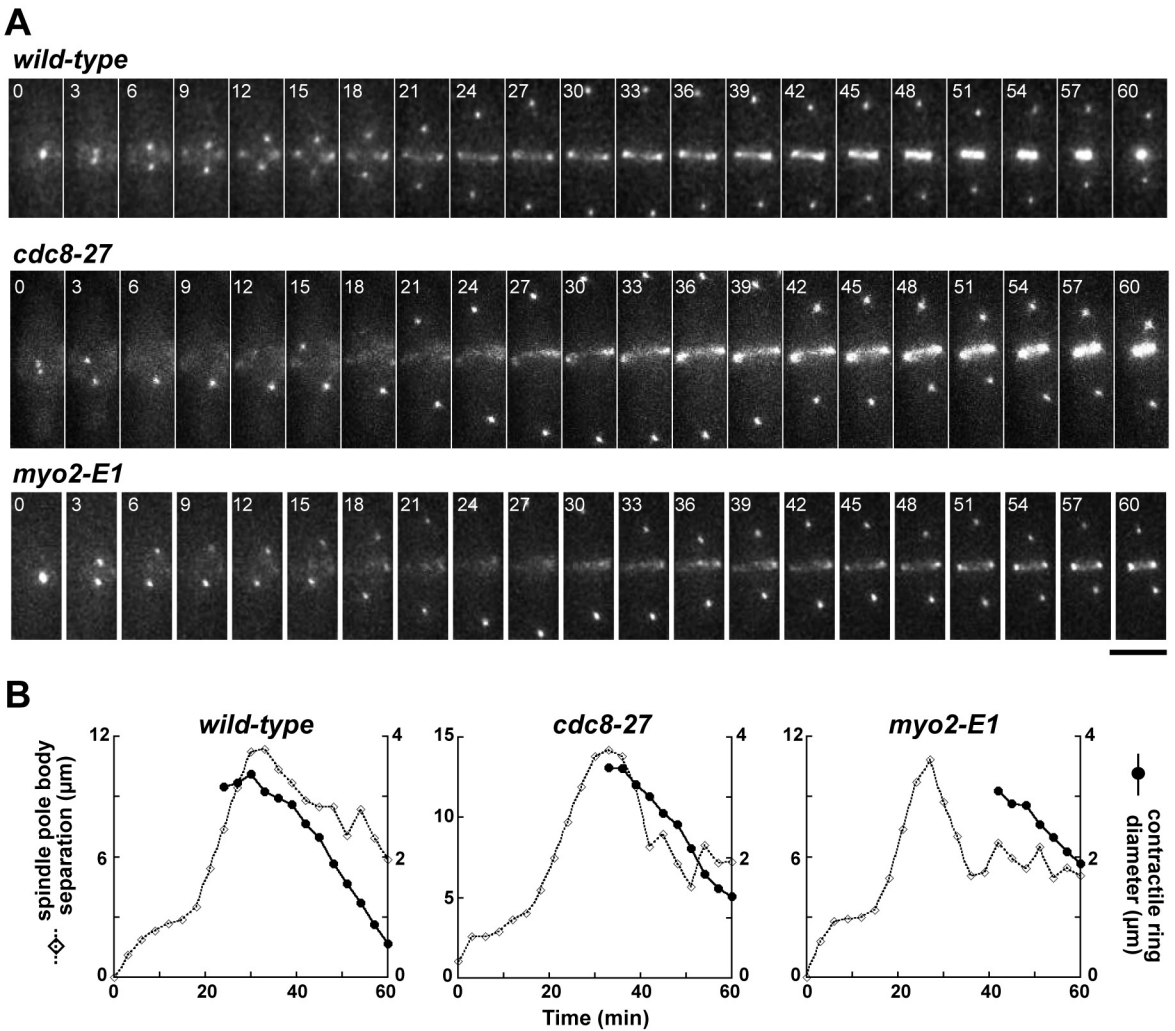

Stark et al.
Figure S3.